

Determination of the resistance across incompressible strips through imaging of charge motion

P. I. Glicofridis, G. Finkelstein,* and R. C. Ashoori

Department of Physics and Center for Materials Science and Engineering, Massachusetts Institute of Technology, Cambridge, Massachusetts 02139

M. Shayegan

Department of Electrical Engineering, Princeton University, Princeton, New Jersey 08544

(Received 18 October 2001; published 13 March 2002)

Using charge-accumulation imaging, we measure the charge flow across an incompressible strip and follow its evolution with magnetic field. The strip runs parallel to the edge of a gate deposited on the sample and forms at positions where an exact number of integer Landau levels is filled. An RC model of charging fits the data well and enables us to determine the resistance across the strip. Surprisingly, we find that the strip becomes more resistive as its width decreases.

DOI: 10.1103/PhysRevB.65.121312

PACS number(s): 73.43.-f, 73.43.Fj, 73.23.-b, 73.40.-c

The edge-state picture of transport in a two-dimensional electron gas (2DEG) in a strong magnetic field appears to explain several key properties of the 2DEG in the quantum Hall effect (QHE) regime. The intersection between the constant Fermi energy and the Landau-level energy near the edge of the 2DEG determines the spatial location of the edge states.¹ In a self-consistent electrostatic picture, edge channels are separated by incompressible strips of integer Landau-level filling.^{2,3} Resulting models involving alternating compressible and incompressible strips have received considerable theoretical and experimental attention.⁴⁻⁶ Several groups have employed local techniques⁷⁻¹³ to resolve the structure of the edge channels.⁷⁻¹² Subsurface charge-accumulation (SCA) imaging enables measurements of both the disorder potential and imaging of low-compressibility strips in the integer QHE.¹¹

In this work, we use SCA to image and characterize the charging properties of the incompressible strips that form in the 2DEG in the presence of a density gradient. The electron-gas charges by pumping charge to it across an incompressible strip. We show here that a simple RC -charging model fits the data well. Using this model we determine the resistance across the strip as a function of magnetic field and find surprisingly, that the strips become more resistive as their widths decrease.

Our samples are made from a standard GaAs/ $\text{Al}_x\text{Ga}_{1-x}\text{As}$ heterostructure with a carrier concentration of $1.5 \times 10^{11} \text{ cm}^{-2}$ and transport mobility of $1.5 \times 10^6 \text{ cm}^2/\text{V sec}$. The 2DEG forms at the GaAs- $\text{Al}_x\text{Ga}_{1-x}\text{As}$ interface 80 nm beneath the surface. We deposited a 10-nm-Cr gate on top of the sample, lithographically patterned in the form of a fingered grating (see schematic in Fig. 1). We scan a sharp Pt-Ir tip to locally probe the sample at a temperature of 0.35 K. Following the initial coarse tip approach, we bring the tip in contact with the gate surface until tunneling current is detected. We repeat this procedure at several locations on top of the gate to determine precisely the tilt of the sample plane. While imaging, we scan the tip just above the gate surface with feedback mechanism switched off. The tip then keeps a safe distance of ≈ 10 nm above the GaAs surface. An ac excitation of 6 mV rms at a frequency of 100 kHz is applied to both the gate and the 2DEG. Due to its capacitance to the

grounded body of the scanning microscope, the 2D electron-layer charges and discharges in response to the applied signal. By measuring the charge induced on the tip, we obtain a charging map of the 2DEG. Both the signal in-phase with and lagging 90° from the ac excitation are recorded using a lock-in amplifier.

Figure 1(a) presents a $12 \times 12 \mu\text{m}$ SCA image at zero magnetic field. These images result from scanning the tip over an ungated portion of the sample situated between two gate fingers that run parallel to each other. The scan window is positioned so that only one finger appears on the left. In the absence of magnetic field, the 2DEG maintains high conductivity and, thus, charges uniformly in phase with the applied ac excitation. As a consequence, the signal lagging the excitation (Y phase) is zero everywhere and the correspond-

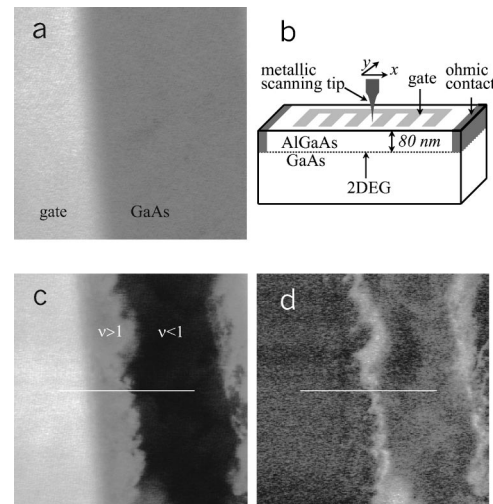


FIG. 1. $12 \times 12 \mu\text{m}$ SCA images, (a) $B=0$ T in-phase signal; (c) 6.4 T in-phase signal and (d) 6.4 T out-of-phase signal; (b) sample schematic. The in-phase images (a) and (c) show the gate (bright region on the left side of the images), which is closer to the scanning probe than the 2DEG, resulting in a larger capacitance signal. Incompressible strips at $\nu=1$ form close to the edge of the gate and separate regions of $\nu < 1$ from those where $\nu > 1$ (sample interior). Another gate sits at $\approx 1 \mu\text{m}$ off to the right of the images. White lines are described in the captions for Figs. 3 and 4.

ing image (not shown) displays no contrast. The picture changes dramatically in applied magnetic field. At 6.4 T (close to filling factor $\nu=1$), charge flowing from the gates, now penetrates the 2DEG only partially [Fig. 1(c)]. In addition, the Y -phase signal in Fig. 1(d) peaks at the boundary between charging and noncharging regions.

In this work, we do not apply any external bias voltage on the gate. However, the electronic density under the metal (chromium) gate is reduced by about 15% from its bulk value due to the difference in chemical potential between the metal and GaAs. As a result of this density profile, at high magnetic fields an incompressible strip, running parallel to each finger, forms in regions where electrons completely fill a Landau level. In these areas $\sigma_{xx} \rightarrow 0$, and the strip prevents charge from flowing freely into the interior of the sample, exactly as depicted in Fig. 1(c). The regions of the 2DEG with very low conductivity give rise to a phase-lagging SCA signal [Fig. 1(d)]. Decreasing the strength of the applied magnetic field reduces the degeneracy of the Landau levels. The strip, as well as the boundary that separates charging from noncharging regions, moves closer to the fingers where the density is lower. By following this evolution with field, we determine that the 2DEG electron density is nearly constant between the gate fingers but decreases closer to the gate. We find a density gradient of $\approx 1.2 \times 10^{10} \text{ cm}^{-2} \mu\text{m}^{-1}$ close to the gate. By moving our scan window laterally along the fingers of the gate, we have verified that neighboring strips may close on each other at certain locations, forming closed loops with the 2DEG inside electrically isolated from the rest of the electron layer.

The work-function difference between the Pt-Ir scanning tip and the GaAs surface results in an electric field that perturbs the electronic density of the 2DEG in the vicinity of the tip. As described elsewhere,¹¹ we perform Kelvin probe measurements and apply a bias voltage to the tip that nulls this electric field. For values away from this nulling voltage, the probe acts as an effective gate on the sample. Figure 2 shows scans of a $12 \times 12 \mu\text{m}$ region at 6.3 T for different tip biases. With the local density under the tip reduced, the condition for integer filling of the $\nu=1$ Landau level is satisfied at a region with higher intrinsic electron density. As a result, the location of the observed strip changes and shifts towards the interior of the imaged region. The resulting density suppression, though local, extends to $\approx 1 \mu\text{m}$ and connects regions that would otherwise be separated by incompressible fluid.

The shapes of areas with high out-of-phase signal in Fig. 2(d) resemble sets of arcs. The centers of the arcs are located roughly along the strip position measured at nulling voltage in Fig. 2(a) suggesting the following nonlocal gating mechanism: bringing the biased tip on-top of a high-density region that does not charge at nulling voltage locally reduces the density and may permit charging. In this case, there must exist a path between the tip location and the gate, where the filling factor is everywhere less than the nearest integer. The density perturbation induced by the tip decays sharply in the lateral direction. Crucial points along this path are situated at the strip location as measured at nulling. Indeed, in many cases the centers of the arcs such as seen in Figs. 2(c) and

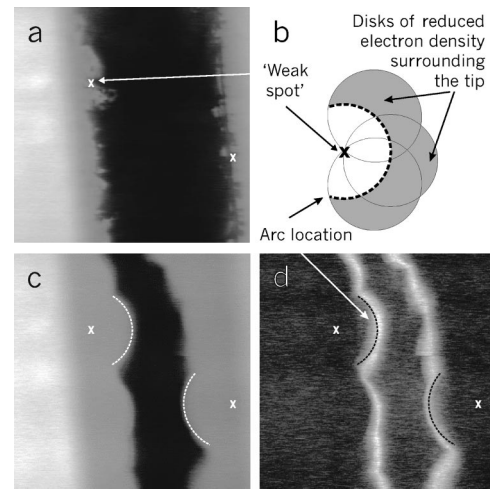


FIG. 2. $12 \times 12 \mu\text{m}$ SCA images at $B=6.3$ T for different biases applied on the tip with respect to the 2DEG. Tip bias V_{tip} is measured in Volts away from the nulling voltage; (a) and (c) present in-phase signal at $V_{tip}=0$ (i.e., nulling) and -1 V, respectively; (d) is the out-of-phase signal corresponding to (c). In (c) and (d), the apparent locations of the incompressible strips at $\nu=1$ are shifted towards the center as the density is lowered by the tip. (b) Shows schematically the origin of the arc shaped features observed in (c) and (d).

2(d), point to the location of features in the unperturbed images [see, for example, the features in Fig. 2(a) marked by “x”]. We postulate that each arc indicates tip locations where the tip influence on a certain “weak link” in the strip is the same.¹² On one side of the arc, the weak link is open and the area under the tip charges fully. On the other side of the arc, the weak link is closed ($\nu>1$) and the area under the tip becomes effectively disconnected from the gate [Fig. 2(b)].

We can counter changes in the position of the strip created with the tip bias by properly tuning the magnetic field. At $\nu=1$, the incompressible strips appear at the same location if we change both magnetic field and tip voltage at a rate of $dV/dB=0.5$ V/T. At $\nu=2$ we find that $dV/dB=1.0$ V/T creates the same effect. This demonstrates that density changes are compensated by varying the number of electrons that each level can accommodate. The voltage required for compensation should be proportional to the filling factor, in agreement with the experiment. All SCA images and measurements reported in this paper, other than those in Figs. 2(c) and 2(d), result from scans taken at nulled tip-sample electric field.

We now describe the results of SCA measurements obtained by scanning the tip along single lines shown schematically in Fig. 1. The boundary between the gate finger and the bare sample occurs at $x \approx 1.5 \mu\text{m}$ (distance of $1.5 \mu\text{m}$ from the leftmost point of the line scan). The magnitude of the resulting signal step reflects the difference in SCA signal measured with the tip positioned above the metal gate ($0 < x < 1.5 \mu\text{m}$) and above a fully charging region of the 2DEG ($1.5 \mu\text{m} < x < 3.1 \mu\text{m}$). This observed step does not vary with magnetic field (see Fig. 3), indicating no field dependence in the amount of charge flowing in regions of the 2DEG adjacent to the gate.

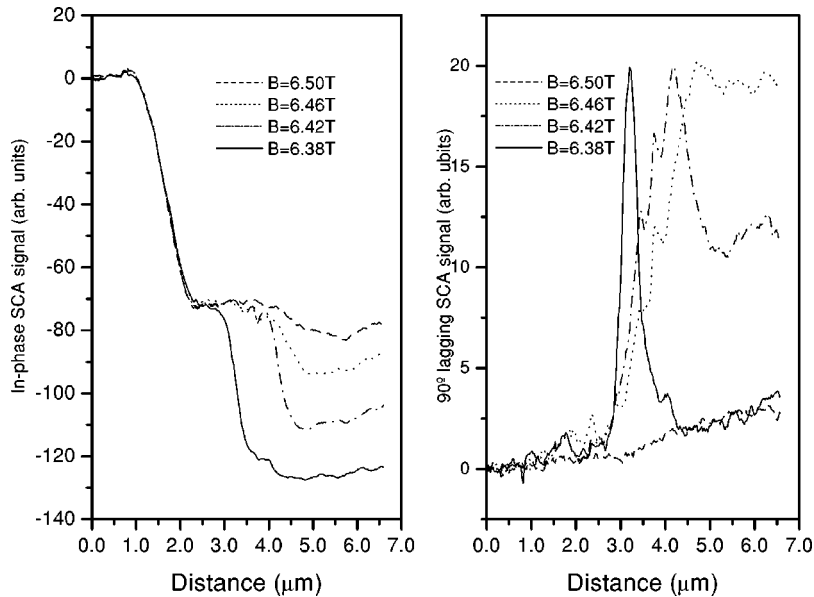


FIG. 3. Evolution of scans taken along the solid white line of Fig. 1 with magnetic field. Note the different vertical scales for the in-phase and out-of-phase curves. Charging of the sample interior becomes less efficient as the field is lowered. The strip is most resistive at 6.38 T where the Y -phase signal goes through a peak and returns again to almost zero level.

At zero magnetic field as well as at fields away from the quantum Hall plateaus, the 2DEG charges nearly as a classical 2D metal. This situation changes upon tuning the field close to the integer Hall plateaus. The leftmost sequence (in-phase signal) of line scans in Fig. 3 shows the appearance and evolution of another SCA signal step at fields around 6.4 T. The decrease in signal in the region between neighboring gate fingers results from the formation of incompressible strips at $\nu = 1$, running parallel to the gate. We point out that this region in the interior, bounded by incompressible strips on both sides, has $\nu > 1$ and high conductivity (σ_{xx}).

To understand the origin of the 90° lagging SCA signal (curves on the right of Fig. 3), we consider an RC charging model for our 2DEG and assume that the interior of the sample charges through a strip characterized by resistance R while the tip is coupled to the 2DEG via a capacitance C (see inset in Fig. 4). As discussed below, this tip-to-sample capacitance totally dominates over the self-capacitance of the “isolated” $\nu > 1$ higher conductivity region, which justifies the use of a lumped circuit model. The model also assumes that the incompressible strip forms the major “obstacle” for charge flow between the gates and the scanning tip. Since the incompressible strips form closed loops surrounding the interior region, similar to Corbino disk geometry, the effective resistance across the strip R should be proportional to $1/\sigma_{xx}$. The resulting in-phase signal measured at the tip, is proportional to $1/[1 + (\omega RC)^2]$ while the out-of-phase evolves as $\omega RC/[1 + (\omega RC)^2]$. The X signal drops steadily to zero as the resistance of the path leading to the region under the tip increases, while the Y signal goes through a peak near the roll-off frequency of $1/(RC)$. The presence of the out-of-phase signal indicates that there is not enough time to fully charge the 2DEG during one complete cycle of the excitation.

Figure 3 shows that the formation of the strip on the high-field side of the Hall plateau ($B = 6.5$ T) begins to impede charging of the interior $\nu > 1$ region of the sample (Fig. 3, distance greater than 4μ). At 6.46 and 6.42 T, we observe a somewhat higher strip resistance, but the interior can still

be partially charged during the ac excitation cycle, as evidenced by a nonzero phase-lagging signal. With decreasing field, the in-phase and phase-lagging signals in the interior $\nu > 1$ region further drop and eventually saturate beyond $B = 6.38$ T. Further reduction of the field simply pushes the strip closer to the edge of the gate and leaves magnitude of the signals in the interior unchanged. We conclude that the resistance across the strip steadily grows as the strip moves closer to the gate, and at $B = 6.38$ T the strip becomes prac-

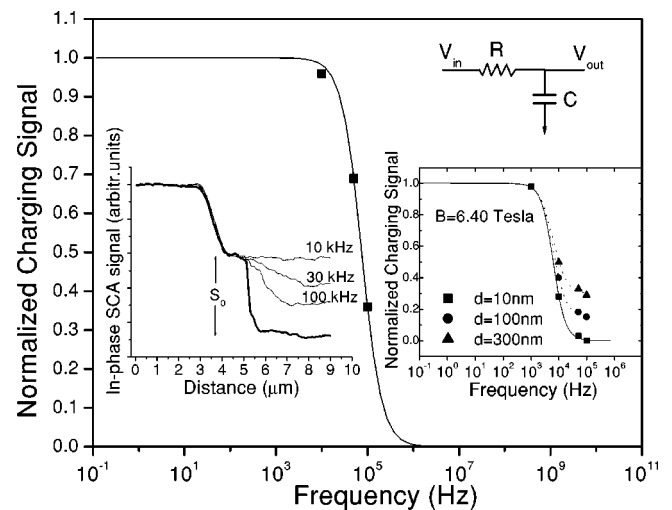


FIG. 4. Frequency dependence of the measured capacitance signal at 6.52 T, as extracted from the traces in the left inset. The solid curve is an RC model fit to the data points. Left inset, in-phase SCA signal from line scans at 10, 30, and 100 kHz. Thick bottom line is frequency independent and corresponds to the sensitivity calibration trace measured at 6.44 T. Data are measured at a different sample location from the one corresponding to Fig. 3. Right inset, degree of charging of the 2DEG measured for different tip-sample separations at 1, 10, 50, and 100 kHz. Data points are derived from line scans at 6.40 T at the same location where measurements for Fig. 3 were taken [solid line in Figs. 1(c) and 1(d)]. Reduction of C_g due to the increase in d leads to faster charging of the electron layer.

tically impenetrable to charge flowing from the gate for excitation frequency of 100 kHz. The density gradient is steeper and closer to the gate and hence the incompressible strips formed there should be narrower.^{3,11} Therefore, the effective resistance for charging across the strip, counterintuitively, is greater for a narrower strip.

The crude RC model used so far dictates that the measured signal also depends upon the excitation frequency. Lowering the measurement frequency should enhance the charging of the 2DEG through the strip provided that R and C remain constant. We show data consistent with this expectation in the left inset of Fig. 4. A line scan at 6.52 T (in a different location from those in Fig. 3), is measured at different frequencies. As expected, the 2DEG charges more fully at lower frequencies, as evidenced by the increased in-phase signal in the $\nu > 1$ region. The lower trace in that inset corresponds to a magnetic field of 6.44 T where the strip allows essentially no charge to cross it. In contrast to line scans taken at slightly higher fields, this trace remains unchanged even at the lowest experimental frequencies.

We use the corresponding step S_0 in the in-phase signal between the fully charged and totally noncharged regions that the strip separates (bold trace in the left inset of Fig. 4), to calibrate the sensitivity of our measurement to full charging. We can, therefore, determine precisely the degree of charging of the 2DEG in the region between the strips at different fields for a range of frequencies and express it as a fraction q of S_0 . Figure 4 plots q against frequency using data from the curves in the left inset. The smooth curve fits the data points using the RC model discussed earlier and works remarkably well. We have performed extensive measurements at several different locations within the sample and find consistent agreement with the RC model.

We can now extract directly the resistance R , of the strip by assuming that the value for C is the known geometric capacitance C_g between the tip and the 2DEG. We justify this assumption below in an examination of the effects of changing the tip-sample separation. C_g is determined by measuring the signal change at zero magnetic field, as we move the tip vertically from “infinity” to within 10 nm from the sample surface, yielding $C_g \approx 0.5$ fF. In addition, since strips form closed loops in our experiment, we are able to follow them to their full extent and hence, measure exactly

their total length. For the fit in Fig. 4 we obtain $RC = 2 \times 10^{-6}$ s and deduce that at 6.52 T ($\nu = 1$), $R_{strip} \approx 100$ M $\Omega/\mu\text{m}$. This resistance increases by 1 order of magnitude to ≈ 1000 M $\Omega/\mu\text{m}$ at $B = 6.48$ T. We find that at a field of 6.44 T, the strip resistivity rises beyond our measurement limit of $\sim 10\,000$ M $\Omega/\mu\text{m}$. The results reproduce consistently at different locations throughout the sample.

We have also measured the strip resistances at $\nu = 2$ and 4. The strip resistivity is ≈ 10 M $\Omega/\mu\text{m}$ at $B = 3.26$ T and ≈ 400 M $\Omega/\mu\text{m}$ at 3.24 T (corresponding to $\nu = 2$). For $B = 1.60$ T ($\nu = 4$), we get $R_{strip} \sim 1$ M $\Omega/\mu\text{m}$. This result follows naturally, since at $\nu = 4$ the energy gap $\hbar\omega_c$ is smaller and the strips should be narrower.³ Temperature-dependent measurements of the strip resistivity, could elucidate the mechanism responsible for charge penetrating the incompressible strip (i.e., electron tunneling or hopping). However, these measurements prove difficult with our apparatus.

The effects of changing tip height are depicted in the right inset of Fig. 4. The corresponding line scans are performed at 6.40 T at the same location as the data set in Fig. 3. The capacitance data points are extracted at the same frequencies for three different tip-sample separations, $d = 10$ nm, 100 nm, and 300 nm. Their strong dependence of charging rates on d implies that the geometric capacitance C_g between the probe and the sample is larger or comparable to the self-capacitance of the region of the 2DEG located to the right of the strip. We obtained similar results for lower-field values up to the point where the strip becomes totally impenetrable. Indeed, $C_{self} \sim \epsilon\epsilon_0 a \sim 1$ fF, with a being a characteristic length scale of the 2DEG region enclosed by the strip (~ 10 μm), is comparable to the value estimated for C_g in our experiment. Consequently, C_g seems to be the relevant parameter in our model and its known value may be used in determining the strip resistance from the product RC_g . From Fig. 4 we also note that, as expected, the 2DEG charges faster as d increases and C_g is reduced.

We would like to thank L.S. Levitov for helpful discussions. This work was supported by the Office of Naval Research, the National Science Foundation DMR, and the Center for Materials Science and Engineering at MIT.

*Present address: Department of Physics, Duke University, Durham, NC 27708.

¹B.I. Halperin, Phys. Rev. B **25**, 2185 (1982).

²A.L. Efros, Solid State Commun. **67**, 1019 (1988); A.M. Chang, *ibid.* **74**, 871 (1990); C.W.J. Beenakker, Phys. Rev. Lett. **64**, 216 (1990).

³D.B. Chklovskii, B.I. Shklovskii, and L.I. Glazman, Phys. Rev. B **46**, 4026 (1992).

⁴S.W. Hwang, D.C. Tsui, and M. Shayegan, Phys. Rev. B **48**, 8161 (1993).

⁵S. Takaoka *et al.*, Phys. Rev. Lett. **72**, 3080 (1994).

⁶N.B. Zhitenev, M. Brodsky, R.C. Ashoori, and M.R. Melloch, Phys. Rev. Lett. **77**, 1833 (1996).

⁷Y.Y. Wei, J. Weis, K.v. Klitzing, and K. Eberl, Phys. Rev. Lett. **81**,

1674 (1998).

⁸K.L. McCormick, M.T. Woodside, M. Huang, M. Wu, P.L. McEuen, C. Duruoz, and J.S. Harris, Phys. Rev. B **59**, 4654 (1999).

⁹A. Yacoby, H.F. Hess, T.A. Fulton, L.N. Pfeiffer, and K.W. West, Solid State Commun. **111**, 1 (1999).

¹⁰G. Finkelstein, P.I. Glicofridis, R.C. Ashoori, and M. Shayegan, Science **289**, 90 (2000).

¹¹G. Finkelstein, P.I. Glicofridis, S.H. Tessmer, R.C. Ashoori, and M.R. Melloch, Phys. Rev. B **61**, R16323 (2000).

¹²M.T. Woodside, C. Vale, P.L. McEuen, C. Kadow, K.D. Maranowski, and A.C. Gossard, Phys. Rev. B **64**, 041310 (2001).

¹³M.A. Topinka *et al.*, Nature (London) **410**, 183 (2001).